Use of Dental Defects Associated with Low-Dose di(2-Ethylhexyl)Phthalate as an Early Marker of Exposure to Environmental Toxicants

Ai Thu Bui, Sophia Houari, Sophia Loiodice, Dominique Bazin, Jérémy Sadoine, Nicolas Roubier, Elsa Vennat, Thu Thuy Tran, Ariane Berdal, Jean-Marc Ricort, et al.

A Section 508–conformant HTML version of this article is available at https://doi.org/10.1289/EHP10208.

Use of Dental Defects Associated with Low-Dose di(2-Ethylhexyl)Phthalate as an Early Marker of Exposure to Environmental Toxicants

Ai Thu Bui,[1] Sophia Houari,[1,2] Sophia Loiodice,[1,2] Dominique Bazin,[3] Jérémy Sadoine,[4] Nicolas Roubier,[5] Elsa Vennat,[5] Thu Thuy Tran,[6] Ariane Berdal,[1,2] Jean-Marc Ricort,[1] Sakina Mhaouty-Kodja,[7] and Sylvie Babajko[1]

[1]Laboratory of Molecular Oral Pathophysiology, Centre de Recherche des Cordeliers, Institut national de la santé et de la recherche médicale Unité mixte de recherche 1138 (Inserm UMRS 1138), Université Paris Cité, Sorbonne Université, Paris, France
[2]Department of Oral Biology, Dental Faculty, Université Paris Cité, Paris, France
[3]Laboratory of Chemistry and Physics, Université Paris-Saclay, Orsay, France
[4]EA 2496 Laboratory of Orofacial Pathologies, Imaging and Biotherapies, Dental School, Université Paris Cité, Montrouge, France
[5]Laboratory of Mechanics of Soils, Structures and Materials, Le Centre national de la recherche scientifique (CNRS), Centrale-Supélec, Université Paris-Saclay, Châtenay-Malabry, France
[5]Institut Curie, Inserm U1196, Université Paris-Saclay, Orsay, France
[6]Faculty of Odonto-Stomatology, Ho Chi Minh University of Medicine and Pharmacy, Ho Chi Minh City, Vietnam
[7]Neuroscience Paris Seine–Institut de Biologie Paris-Seine, CNRS, Inserm, Sorbonne Université, Paris, France

Background: Markers of exposure to environmental toxicants are urgently needed. Tooth enamel, with its unique properties, is able to record certain environmental conditions during its formation. Enamel formation and quality are dependent on hormonal regulation and environmental conditions, including exposure to endocrine disrupting chemicals (EDCs). Among EDCs, phthalates such as di-(2-ethylhexyl) phthalate (DEHP) raise concerns about their contribution to various pathologies, including those of mineralized tissues.

Objectives: The effects of exposure to low-doses of DEHP on the continually growing incisors were analyzed in mouse males and females.

Methods: Adult male and female C57BL/6J mice were exposed daily to 0.5, 5, and 50 μg/kg per day DEHP for 12 wk and their incisors clinically examined. Incisors of males were further analyzed by scanning electron microscopy (SEM), micro X-ray computed tomography (micro-computed tomography; μCT), and nanoindentation for the enamel, histology and real-time quantitative polymerase chain reaction (RT-qPCR) for the dental epithelium.

Results: Clinical macroscopic observations of incisors showed various dose-dependent dental lesions such as opacities, scratches, and enamel breakdown in 30.5% of males (10 of 34 total incisors across three independent experiments), and 15.6% of females (7 of 46 incisors) at the highest dose, among which 18.1% (6 of 34 total incisors across three independent experiments) and 8.9% (4 of 46 incisors), respectively, had broken incisors. SEM showed an altered enamel surface and ultrastructure in DEHP-exposed male mice. Further characterization of the enamel defects in males by μCT showed a lower mineral density than controls, and nanoindentation showed a lower enamel hardness during all stages of enamel mineralization, with more pronounced alterations in the external part of the enamel. A delay in enamel mineralization was shown by several approaches (μCT, histology, and RT-qPCR).

Discussion: We conclude that DEHP disrupted enamel development in mice by directly acting on dental cells with higher prevalence and severity in males than in females. The time window of DEHP effects on mouse tooth development led to typical alterations of structural, biochemical, and mechanical properties of enamel comparable to other EDCs, such as bisphenol A. The future characterization of dental defects in humans and animals due to environmental toxicants might be helpful in proposing them as early markers of exposure to such molecules. https://doi.org/10.1289/EHP10208

Introduction

The environment is continually evolving, with considerable changes in recent decades that have had an impact on human health and well-being, as well as all living organisms.[1–4] Markers of exposure to environmental toxicants are urgently needed and could include tooth enamel.[5,6] Enamel is the hardest biomineralized tissue; it is composed of ∼97% hydroxyapatite crystallites, forming a typical prismatic structure.[7] Its unique properties allow the retrospective evaluation of environmental conditions, either by direct detection of pollutants entrapped in the enamel mineral[6] or by indirect characterization of enamel defects related to alterations in cell activity during enamel formation.[8] Enamel formation follows the well-known spatial-temporal sequence of ameloblast proliferation, differentiation, maturation, and death.[7,9,10] Briefly, after stem cell commitment in the cervical loop, secretory-stage ameloblasts secrete enamel matrix proteins (EMPs) that determine enamel thickness, and maturation-stage ameloblasts secrete proteases, and control pH and ion transports, allowing apatite crystal assembly and complete enamel mineralization. Ameloblasts disappear during tooth eruption. Thus, any disruption of ameloblast activity leads to irreparable enamel defects that may be used for recording ameloblast stressors.

The continually growing rodent incisor model allows the investigation on amelogenesis in adult animals, in contrast to humans, for whom amelogenesis occurs during a fixed time-window, from the fetal stage to 6–8 years of age.[11] Amelogenesis is controlled by endogenous transcription and growth factors.[12] In addition, ameloblasts express many hormone receptors, including those for growth hormone,[13] vitamin D,[14] estrogens, and androgens,[15–17] as well as for most steroids.[18] These receptors and their ligands modulate the expression of genes involved in enamel mineralization in humans[19] and rats.[17] Amelogenesis may thus be irreversibly altered by agents that interfere with these hormone pathways, such as endocrine disrupting chemicals (EDCs) widely present in the environment.[20] Exposure to EDCs is associated with many chronic pathologies for which males and females may show different susceptibility.[21,22] Exposure to EDCs, such as polychlorinated biphenyls,[23] dioxin,[24] and bisphenol A (BPA),[25] has already been associated with enamel

Address correspondence to Sylvie Babajko, Centre de Recherche des Cordeliers, Inserm UMRS 1138, 15 rue de l'Ecole de Médecine, Paris 75006 France. Telephone: 33 1 44 27 55 82. Email: sylviebabajko@gmail.com

Supplemental Material is available online (https://doi.org/10.1289/EHP10208).

A.T.B. is a recipient of funds from the French Ministry of Higher Education, Research, and Innovation. The authors declare that they have no actual or potential competing financial interests.

Received 26 August 2021; Revised 4 May 2022; Accepted 9 May 2022; Published 22 June 2022.

hypomineralization. These factors, alone or in combination, may contribute to or aggravate developmental defects of enamel (DDEs).[26] Among EDCs, phthalates, in particular di-(2-ethylhexyl)phthalate (DEHP), constitute an important family of active molecules present in food containers, plasticizers, consumer goods, toys, cosmetics, and medical devices.[27] Newborns and children are sensitive to DEHP, as suggested in a study of six premature infants on intravenous infusion who showed higher levels of DEHP compared with the U.S. general population.[28] Despite regulations and bans, DEHP may still be present in many medical devices and equipment in neonatal intensive care units, as suggested by a study of 97 devices from two hospitals in Belgium and the Netherlands,[29] which may lead to high DEHP contamination of hospitalized children with a long length of stay.[30,31] The tolerated dose intake (TDI) accepted in Europe has been reduced to 50 μg/kg per day,[32] whereas the reference dose in the United States is 20 μg/kg per day.[33] Given the widespread presence of DEHP, the potential contamination by DEHP of children (with ongoing formation of teeth), and previous data on the effects of EDCs on enamel, as well as those of DEHP on bone mineralization,[34] we explored the potential dental effects of DEHP in the continually growing incisor of adult mice chronically exposed to low-dose DEHP. In this study, we aimed to characterize the impact of DEHP on enamel structure using scanning electron microscopy (SEM), micro X-ray computed tomography (micro-computed tomography; μCT) and nanoindentation analyses, as well as on dental epithelial cells using histology and real-time quantitative polymerase chain reaction (RT-qPCR) analyses. Experimental data on mice could be useful in improving our understanding of the effects of EDCs in humans, for whom amelogenesis is a time-limited process.

Methods

Animals, Treatments, and Sample Collection

Studies were performed in accordance with the French and European legal requirements (Decree2010/63/UE)[35] and were approved by the Charles Darwin Ethical Committee (project no. 01490.02). All animals were treated humanely and with regard toward the alleviation of suffering. These animals were part of a larger study on reproductive behavior in males[36] and females.[37] Eight-week-old C57BL/6J male and female mice (Janvier) were housed in nest-enriched polysulfone cages, maintained at 22°C/50% relative humidity and under a 12:12 h light-dark cycle, fed a standard diet (A03-10; Safe-diets), adhering to the Animal Research: Reporting of *In Vivo* Experiments (ARRIVE) guidelines, as previously described.[36,37] To mimic the major route of exposure, DEHP (Sigma-Aldrich) was dissolved in ethanol and water (1% and 40% of prepared food, respectively) and incorporated by the experimenter into powdered food (A03-10; Safe-diets) that was then reconstituted into pellets, as previously described.[36,37] Mice were fed *ad libitum* for 12 wk with chow containing the vehicle [control (C) group] or DEHP such that the exposure was equivalent to a TDI dose of 50 (D-50 group), 5 (D-5 group), or 0.5 μg/kg body weight (BW) per day (D-0.5 group). Mice were weighed weekly, and DEHP doses were adjusted to their BWs and calculated for a daily food intake of 5 g per animal. Reconstituted pellets were prepared every week immediately after animal weighing, stored at 4°C, and changed twice a week. All doses of exposure to DEHP were thus equivalent to or lower than the TDI of 48 μg/kg BW per day established by the European Food and Safety Agency[32] on the basis of the ability of this molecule to reduce fetal testosterone production.

The data presented here were obtained with a total of 54 intact males and 66 females intact or ovariectomized and primed with estradiol and progesterone to normalize hormonal levels.[37] Female mice were ovariectomized under general anesthesia (xylazine 10 mg/kg and ketamine 100 mg/kg). At the time of ovariectomy, all females received 1-cm subcutaneous Silastic implants (3.18-mm outer diameter × 1.98-mm inner diameter; Dow Corning) filled with 50 μg of estradiol benzoate (Sigma-Aldrich) in 30 μL sesame oil and sealed at each end with Silastic adhesive, as previously described.[36,37] Each female was given a subcutaneous injection of 1 mg/100 μL progesterone (Sigma-Aldrich) dissolved in sesame oil 4–5 h before analyses. Animals were divided into three independent series of experiments for each sex, with at least five animals per group (Table S1). At the end of the treatment, 20-wk-old animals were euthanized (after 12 wk of exposure), using pentobarbital injection (120 mg/kg) and immediately processed for the collection of biological samples.

Hemimandibles were either fixed in 4% paraformaldehyde for further structural analyses (same incisors were used for all the structural analyses) or freshy dissected. All incisors were independently examined by two investigators. Incisors were micro-dissected from hemimandibles under a binocular stereoscope (Leica MZFIII; Mayers). Epithelium layers containing ameloblasts were collected while carefully maintaining the incisors intact for structural analyses.

Scanning Electron Microscopy

The surface of the teeth was gently cleaned manually with a sheet of Kleenex tissue and ultrasonicated (Branson 200; Sigma-Aldrich) for 5 min to remove residual attached tissues. Images of the surface microstructure were obtained using a Zeiss SUPRA55-VP electron microscope. To maintain sample integrity, measurements were conducted at low voltage (between 0.5 and 2 kV) without the usual sample surface coating.[38] Three regions of interest (ROI) were distinguished, two from the erupted incisor (tip and early erupted part) and one located under the first molar corresponding to early-maturation stage enamel.

Micro X-Ray Computed Tomography

Incisors were imaged by μCT (Quantum FX Caliper, Life Sciences; Perkin Elmer). The acquisition parameters were a 10 × 10 mm field of view, 20–μm voxel size, 90 kV, 160 μA, 360° rotation, and 3-min exposure time for the X-ray source. Then, 360° projections were reconstructed using RigakuSW (Caliper) software into a 512 × 512 × 512-voxel matrix. Stacks of images were oriented for choosing similar ROIs across samples, distinguishing secretory and maturation stages based on anatomical landmarks,[39] processed using DataViewer software [Skyscan (release 1.5.2.4; Kontich)], and finally analyzed using the CT-Analyser software [Skyscan (release 1.13.5.1; Kontich)]. Image densities were scaled in Hounsfield Units (HUs) during acquisition and converted to mineral density (equivalence in milligrams of hydroxyapatite per cubic centimeter) during postprocessing. Quantitative analysis focused on three 500–μm-thick ROIs in early- and late-maturation stage enamel (illustrated in the corresponding figures), determined using the eruption point, the relative size of the pulp chamber, and the first and second molar position as references. A threshold was applied to separate enamel from other tissues and mineral density calculated for each ROI. For the control groups, two incisors per set of experiments were scanned ($n = 6$). For the D-50 groups, more incisors ($n = 12$) were chosen randomly among both phenotypes, including intact and light and severely affected teeth from three sets of experiments because of the loss of certain ROIs. ROIs were independently selected twice to calibrate the scanning data ($n_{ROI} = n \times 2$).

Nanoindentation

Nanoindentation was performed on frontal sections of mouse incisors dehydrated in ethanol for 48 h at 4°C, as previously described.[40] A minimum of three teeth per condition were embedded in epoxy resin (Epofix A8; Struers). The first slice was cut along the axial plane at the erupted point using a rotating diamond wheel (Isomet Diamond

15 HC; Buehler) to analyze late mature enamel. Then, the block containing the rest of the incisor was reoriented and cut along the sagittal plane to localize and analyze early mature enamel. The surface was polished using progressively finer polishing media (SiC papers followed by diamond down to 1 μm) and, finally, cleaned in a deionized water ultrasonic bath (Branson 200; Sigma-Aldrich). The indentation experiments were performed using a calibrated Berkovich nanoindenter [XP; MTS System Corporation, with a continuous stiffness module (CSM module)]. A minimum of 90 indent locations per slice were defined for each sample. Indent spacing was set to 15 μm and the indentation depth set to 1 μm. Elastic moduli and hardness were obtained by averaging the values from the CSM module, between a minimal (600 nm) and a maximal (950 nm) depth. Images of the surfaces were captured before and after indentation (Infinite Focus microscope; Alicona).

Masson's Trichrome Staining

Hemimandibles were immediately fixed after dissection in 10% formalin for 48 h and were decalcified with 4.13% ethylenediaminetetraacetic acid (Sigma-Aldrich) in phosphate-buffered saline for 4 wk at 4°C. Samples were dehydrated in increasing concentrations of ethanol and, finally, embedded in paraffin. Hemimandibles were longitudinally oriented, and 7–μm-thick serial sections cut using a rotary microtome (Leica RM 2135). Serial sections were stained with hematoxylin–eosin (HE) for determination of the cell morphology and stage of amelogenesis. Slices presenting secretory and maturation stages with a well-determined transition landmark were selected for further analyses. Rehydrated sections were successively incubated for 5 min with iron hematoxylin, 0.05% lithium carbonate in fuchsin acid, 5% phosphomolybdic acid solution, and, finally, light green dye. Slices were finally reimmersed in Clearene (Leica 3803620) and mounted in drops of xylene-based mounting resin. Histochemical visualization was performed using a bright-light microscope with a digital camera and image capture software (Leica DM2500P).

Five slices for each group of animals (C, D-5, and D-50) were randomly selected and used for calculation of the number of ameloblasts in the transition stage. The percentage of nonmineralized enamel in the transition stage was evaluated for the total enamel thickness in three different areas.

Cell Cultures and Treatments

The rat ameloblastic cell line HAT-7,[41] established from the cervical loop of rat incisors, was provided by Pr. H. Harada (Iwate Medical University, Japan) and cultured as previously described.[25] Briefly, cells were cultured in Dulbecco's Modified Eagle Medium, Nutrient Mixture F12 (DMEM/F-12; GIBCO BRL), supplemented with 10% fetal bovine serum (FBS), 100 U/mL penicillin, and 100 U/mL streptomycin. Twelve hours before the treatments, 2×10^5 cells/well (∅ 35 mm) were seeded in DMEM/F-12 without phenol red (GIBCO BRL) containing 10% charcoal-treated FBS, 100 IU/mL penicillin and 100 μg/mL streptomycin. Treated cells were cultured in the same medium without FBS, containing 10^{-10} to 10^{-4} M mono (2-ethylhexyl) phthalate (MEHP; Sigma-Aldrich) (which is a DEHP metabolite) or an equivalent volume of 0.1% dimethyl sulfoxide (vehicle), for 48 h.

Total RNA Extractions and RT-qPCR Analysis

Total RNA was isolated from micro-dissected epithelia and cultured cells using a silica membrane following the manufacturer's instructions (RNeasy Mini Kit; Qiagen). One microgram of total RNA

Table 1. List and sequences of primers used for RT-qPCR analyses.

Genes	Species	Primer sequences
Amelx (amelogenin)	m	5′-AAGCATCCCTGAGCTTCAGA-3′
		5′-ACTGGCATCATTGGTTGCTG-3′
Ambn (ameloblastin)	m	5′-AGCTGATAGCACCAGATGAG-3′
		5′-GAACAGAGTTCCATAGGCCA-3′
Enam (enamelin)	m	5′-TCCTTGTTTTCCTGGGTCTG-3′
		5′-ATCCATTGGGTACTGGTGGA-3′
	r	5′-CATGTGGCCTCCGCCAGTCC-3′
		5′-GTCATCTGGGGGCGGGTCCT-3′
Amtn (amelotin)	m	5′-GGACAGCAACAGCTGCAA-3′
		5′-TGTGAAGATTTGGGAGGCTAA-3′
Mmp20 (matrix metalloproteinase 20)	m, r	5′-CTGGGCCTGGGCCATTCCAC-3′
		5′-CTGGTGATGGTGCTGGGCCG-3′
Klk4 (kallikrein-related peptidase 4)	m	5′-GCATCCGCAGTGGGTGCTGT-3′
		5′-CACACTGCAGGAGGCTGGGC-3′
Slc24a4 (solute carrier family 24, member 4)	m	5′-ACGGAGATGTCGGTGTAGGA-3′
		5′-CAATGGCACAGAAGGGTCGT-3′
Slc26a4 (solute carrier family 26, member 4)	m	5′-CGGAGCCCAAACAGGTGG-3′
		5′-CCAAAGGCTCTCTTTCTTGAGC-3′
Slc5a8 (solute carrier family 5, member 8)	m	5′-ACGGTGGAACTGATAACCCG-3′
		5′-GAAGCTTCACAAGCGAGTCC-3′
AR (androgen receptor)	m	5′-ACCTGACCTGGTTTTCAATGAGTATC-3′
		5′-GTTATCTGGAGCCATCCAAACTCTT-3′
*ER*α (estrogen receptor alpha)	m	5′-AAGAGAGTGCCAGGCTTTGG-3′
		5′-ACGTAGCCAGCAACATGTCA-3′
	r	5′-CCAGCTACAAACCAATGCACCATC-3′
		5′-GGTCTTTTCGTATCCCGCCTTTC-3′
Gapdh (glyceraldehyde-3-phosphate dehydrogenase)	m, r	5′-GACCCCTTCATTGACCTCAACTAC-3′
		5′-AAGTTGTCATGGATGACCTTGGCC-3′
Rs15 (ribosomal protein S15)	m, r	5′-GGCTTGTAGGTGATGGAGAA-3′
		5′-CTTCCGCAAGTTCACCTACC-3′
Tbp1 (TATA-binding protein 1)	m	5′-AGCTCTGGAATTGTACCGCA-3′
		5′-AATCAACGCAGTTGTCCGTG-3′
	r	5′-CACGAACAACTGCGTTGATC-3′
		5′-TTTTCTTGCTGCTAGTCTGGAT-3′

Note: m, mouse; r, rat; RT-qPCR, real-time quantitative polymerase chain reaction.

quantified using a Qubit fluorometer (Thermo Fisher Scientific) was used for the reverse transcription reaction using Superscript II enzyme (Invitrogen) and specific primers (Eurogentec) (Table 1). Forty cycles of RT-PCR (30 s denaturation at 95°C, and 60 s for annealing and extending at 60°C) were performed using a CFX96 RT-PCR detector system with the dye Kapa SYBR Green fluorescence (CliniSciences). Nonspecific signals were checked using melting curves. Results were then normalized with the expression levels of three reference genes [glyceraldehyde-3-phosphate dehydrogenase (*Gapdh*), Ribosomal protein S15 (*Rs15*), and TATA-binding protein 1 (*Tbp1*)].

Statistics

Results are expressed as means ± standard deviations (SDs) and were analyzed using one-way analysis of variance (ANOVA) with a post hoc test for multiple comparisons with Tukey's correction (GraphPad 9 software; version 9.0.0) and Mann-Whitney tests for single comparison. The diagnosis and recording of dental defects were carried out for both males and females. Further enamel analyses (SEM, µCT, nanoindentation, and histology) were carried out in males only, using the same incisors for all mineral analyses (µCT was the first, nanoindentation the last). For calculation of percentage affected and broken incisors, the percentage per each individual experiment replicate was calculated and then the mean of those percentages was taken (Table S1). All data were obtained with at least three independent series of experiments. Values were considered to be significantly different when $p \leq 0.05$, and highly significantly different when $p \leq 0.01$ or $p \leq 0.001$.

Results

Tooth Integrity in Mice Exposed to DEHP

Macroscopic observation of mouse incisors under a magnifying glass showed dental defects in males and females exposed to DEHP (Figure 1A). Lesions included broken incisors, yellowish

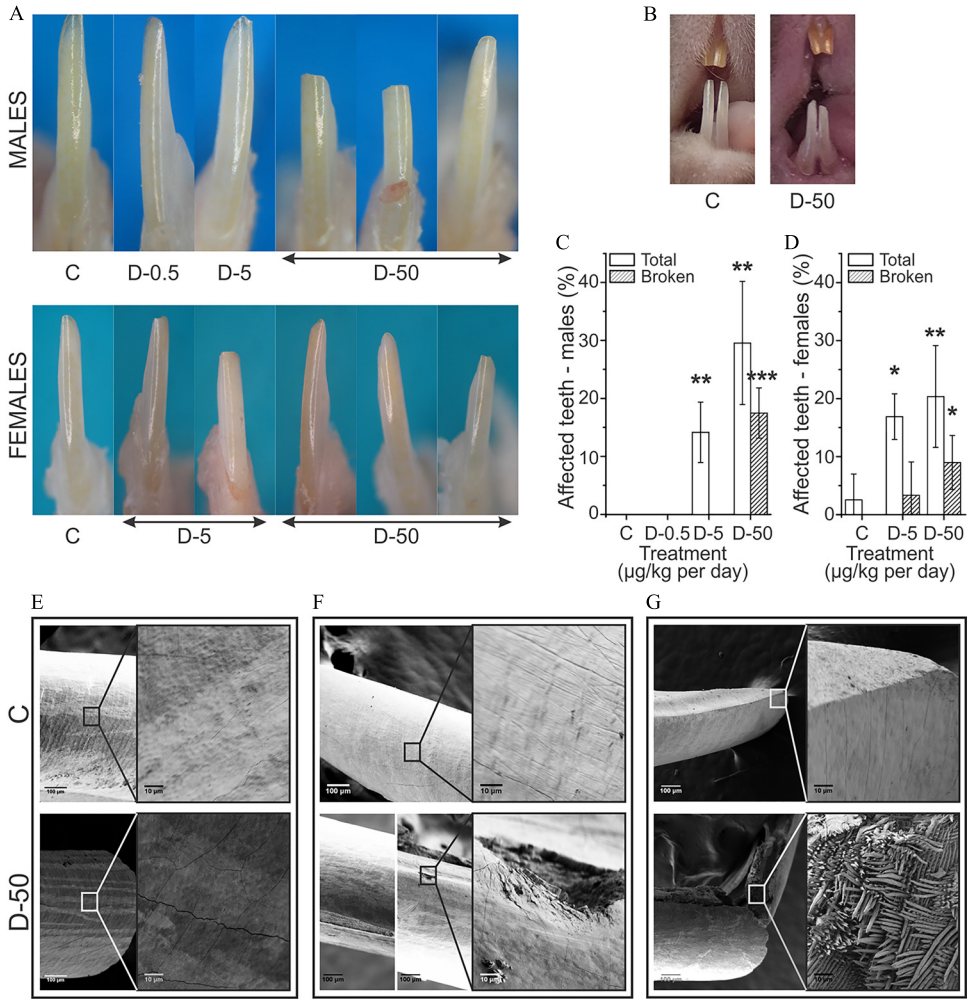

Figure 1. Comparison of dental defects in male and female mice exposed to DEHP for 12 wk. (A) Male and female mouse incisors treated with 0, 0.5, 5, or 50 µg/kg BW per day DEHP (control, D-0.5, D-5, D-50, respectively) observed and photographed under a binocular magnifying glass (Leica MZFIII; Mayers). All incisors were independently examined by two investigators and sorted according to the presence or absence of defects. (B) Direct observation of mouse incisors in the oral cavity. (C) Mean percentage of all dental defects in males, including altered incisors (chipped, opaque, and broken) (white bars) and broken incisors only (hatched bars). (D) Mean percentage of all dental defects in females, including altered incisors (chipped, opaque, and broken) (white bars) and broken incisors only (hatched bars). The data are expressed as the mean percentage (± SD) measured in a total of 15–24 animals per group distributed among three independent experiments with at least five animals per group for each series, except for the D-0.5 male group, which was tested once only ($n = 5$) (Table S1 for details). One-way ANOVA analyses with post hoc tests for multiple comparisons with Tukey's correction (*, $p < 0.05$, **, $p < 0.01$, ***, $p < 0.001$ vs. the control group) are indicated. Scanning electron microscopy (SEM) analysis of the surface of early erupted enamel covered by the alveolar crest of (E) control and (F) DEHP-treated (D-50) male incisors (scale bar: 100 µm for the large view; scale bar: 10 µm for the magnification). (G) SEM analysis of the enamel surface of incisor tips of a control male and a D-50 male. Summary data for (C) and (D) available in Table S1. Note: ANOVA, analysis of variance; C, control; DEHP, di-(2-ethylhexyl) phthalate; SD, standard deviation.

or whitish opacities, as well as chipped teeth with enamel breakdown. In severe cases, the defect could be detected directly in the oral cavity (Figure 1B).

Dose-dependent defects were observed in male mice, with a higher prevalence and severity in the D-50 groups than in the D-5 groups. No defects were detected in the D-0.5 group nor in controls (Figure 1A,C). A mean of 30.5% of incisors of males exposed to D-50 (10 of 34) presented opacities, scratches, or enamel breakdown, with 18.1% (6 of 34) of broken incisors (Figure 1C; see Table S1 for further details for calculation of mean percentages) associated with opacities. In the D-5 groups, only 15.6% (5 of 32) of incisors were altered, with none broken.

Defects among females occurred with a lower frequency and were less severe than in males (Figure 1D; Table S1). A mean of 16.9% (8 of 48) and 15.6% (7 of 46) of incisors of females exposed to D-5 and D-50 were affected, and 3.3% (2 of 48) and 8.9% (4 of 46) were broken, respectively (Table S1).

Enamel surfaces of control and DEHP-treated male incisors were analyzed by SEM. The control incisors were completely devoid of any significant defect, whereas the teeth of male mice exposed to D-50 showed shallow cracks and peeling enamel in numerous locations (0–3/incisor) (Figure 1E–G). The number and the surface of defects depended on the tooth analyzed.

Enamel Mineral Density in Male Mice Exposed to DEHP

Dental mineralization defects were observed on the incisors of DEHP-treated mice by µCT for both transition (Figure 2A) and maturation regions (Figure 2B,C). Enamel mineral density was quantified in three 500–µm-thick ROIs (identified as ROIs A, B, and C) (Figure 2C). ROI A corresponded to nonerupted enamel covered by alveolar bone and located 2 mm from the alveolar crest, ROI B corresponded to just-erupted enamel at alveolar crest, and ROI C was close to the tip. In control mice, the mean mineral density did not vary significantly from one ROI to another and was equivalent to $516.3 \pm 14.6\,mg/cm^3$ with nondispersed points of quantification (Figure 2D; Table S2). In D-50 groups, enamel mineral density was significantly lower in all three ROIs compared with the corresponding control ROIs, with the highest difference for ROI C. Because 18.1% (6 of 34) of males in the D-50 groups showed broken incisors, there were fewer opportunities to analyze ROIs B and C than ROI A. The remaining tip incisors showed overall 10% lower mineral density (471.2 vs. 516.0 mg/cm^3 for ROI B and 462.8 vs. 514.3 mg/cm^3 for ROI C), whereas the difference was only 5% (492.2 vs. 518.7 mg/cm^3) in ROI A but still significant. When broken and intact incisors were distinguished (see Figure S1A for details), the mean mineral density of intact-tip incisors in ROI A was higher ($506.1 \pm 20.8\,mg/cm^3$) than that of incisors with broken tips ($480.5 \pm 30.5\,mg/cm^3$). Thus, the 2% difference between intact incisors (of the D-50 group) and controls (506.1 vs. 518.7 mg/cm^3) was not statistically different ($p = 0.09$), whereas the 8% difference between the mineral density of broken incisors in D-50 group and controls (480.5 vs. 518.7 mg/cm^3) was significative ($p < 0.01$) (Figure S1A and Table S2). The early maturation region of nonerupted enamel showed no significant differences between the control and D-50 groups (Figure S1B), with a mean density of 498 ± 24 and $500 \pm 25\,mg/cm^3$, respectively (Table S3). Careful qualitative analyses of µCT images did not allow us to detect obvious differences in oral bone mineralization between the mandibles of D-50 groups and the controls (Figure 2A–C).

Timing of Incisal Enamel Mineralization Process in Male Mice Exposed to DEHP

The enamel mineralization process from the late secretory to the transition stage was evaluated at the same two positions, at the distal root of the second molar (Figure 2A) and of the first molar (Figure 2B), respectively. µCT analysis of incisal enamel located on the second molar section showed hypomineralyzed enamel, in gray on captured images, in D-50-groups of mice, whereas control enamel in the same section was white, showing higher mineralization (Figure 2A). Careful observations of µCT images suggested that the volume of the pulp chamber appeared to be greater in incisors of D-50-treated male mice than in controls in the same section (Figure 2A–C).

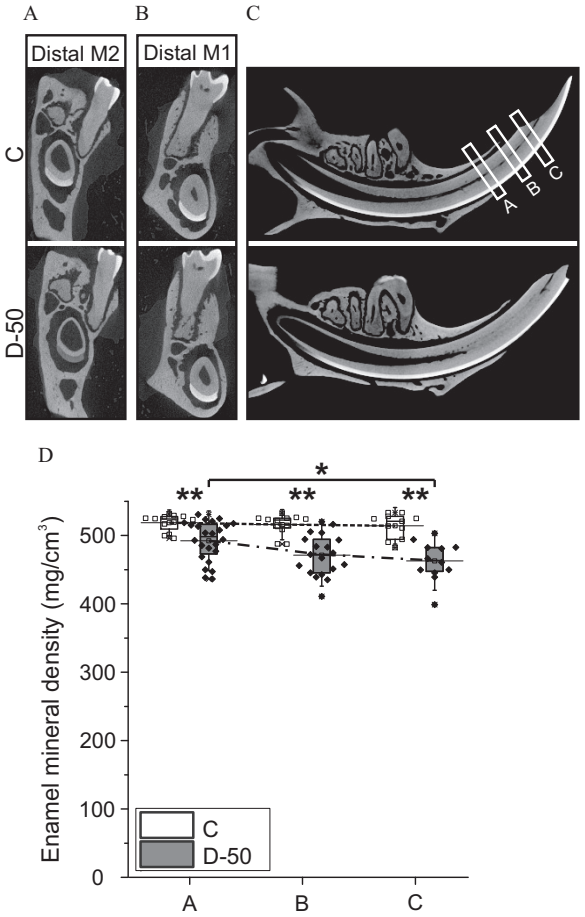

Figure 2. Control and DEHP-treated male mouse enamel analysis by µCT. (A) Frontal slices passing through the distal root of the second molar (M2). In the incisor under M2, enamel appeared as the most mineralized white structure in the control group, and as a gray structure in the DEHP-treated (D-50) group. This region corresponds to the transition stage of amelogenesis. (B) Frontal slices passing through the distal root of the first molar (M1). (C) Saggital slices through the length of the incisor showing the continuing enamel formation with the most mature and mineralized enamel in the erupted incisor (in the right part of the photo). Positionning of the three 500–µm-large ROIs—ROI A: nonerupted enamel block located 2 mm from the alveolar crest; ROI B: just-erupted enamel at the alveolar crest; and ROI C: block of the tip 2 mm away from the crest. (D) Quantification of enamel mineral density of control mice, in the white box ($n = 6$ incisors, and ROIs independently selected twice to calibrate the scanning data), and DEHP-treated enamel (D-50), in the gray box ($n = 12$ incisors). Among them 6 were broken, and ROIs were independently selected twice to calibrate the scanning data) in three ROIs: ROI A, B, and C (Figure S1 for details). Values were considered to be significantly different vs. controls (*) when $p < 0.05$ and highly significantly different (**) when $p \leq 0.01$. Boxes present values as 25th and 75th percentiles, with error bars for SDs, and midlines for the mean values. Mann-Whitney tests were used for single comparisons between control and D-50 groups. Summary data for (D) are available in Table S2. Note: C, control; DEHP, di-(2-ethylhexyl) phthalate; µCT, microcomputed tomography; ROI, region of interest; SD, standard deviation.

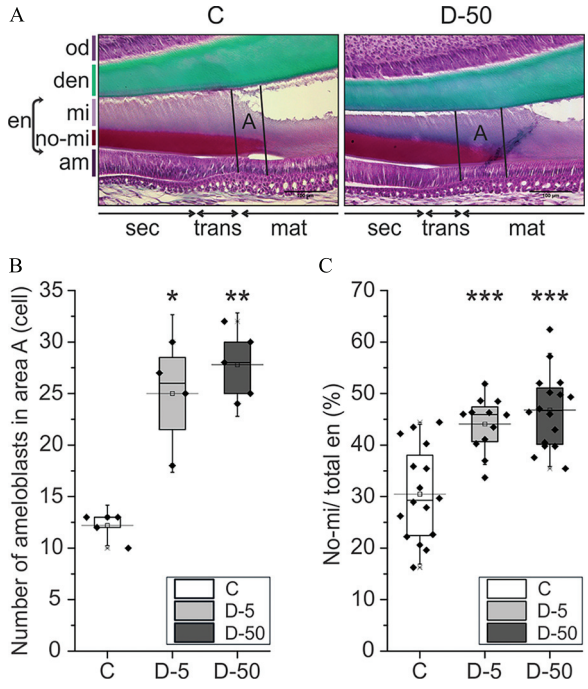

Figure 3. Comparison of dental epithelium histology of control and DEHP-treated male mice. (A) Comparison of dental epithelium organization in the transition stage of amelogenesis between control mice and mice exposed to 50 µg/kg BW per day DEHP (D-50). Fixed demineralized mouse mandibles were stained by Masson's trichrome coloration showing nonmineralized enamel (no-mi) in red, dentin (den) in green, and cells in purple. (B) Number of ameloblasts counted in area A limited by the end of the transition stage and ameloblasts in the early-maturation stage corresponding to the end of nonmineralized enamel–matrix ($n = 5$ for control group, $n = 4$ for D-5 group, $n = 5$ for D-50 group). (C) Ratios of nonmineralized enamel on the total thickness of enamel measured at the transition stage in C, D-5, and D-50 groups. For each incisor, three areas of transition stage were selected including the mid-transition, 50 µm before the mid-transition (which corresponded to the late-secretory stage), and 50 µm away from the mid-transition (which corresponded to the early-maturation stage). Values were considered to be significantly different vs. controls (*) when $p \le 0.05$ and highly significantly different (**) when $p \le 0.01$ or (***) $p \le 0.001$, using one-way ANOVA analyses with post hoc tests for multiple comparisons with Tukey's correction. Boxes present values as 25th and 75th percentiles, with error bars for SDs and midlines for the mean values. Summary data for (B) and (C) available in Tables S4 and S5, respectively. Note: am, ameloblast; ANOVA, analysis of variance; BW, body weight; C, control; DEHP, di-(2-ethylhexyl) phthalate; den, dentin; en, enamel; mat, maturation stage; mi, fully mineralized enamel; no-mi, nonmineralized enamel–matrix; od, odontoblast; SD, standard deviation; sec, secretory stage; trans, transition stage.

We then carefully analyzed the histology and initiation of the mineralization process by Masson's trichrome colorations, with a focus on transition stage ameloblasts (Figure 3A). The total number of ameloblasts counted in the transition stage was the same or slightly higher in DEHP-treated mice than in controls, with 22.6 ± 2.8 cells for the control group and 25.2 ± 4.3 cells for the D-50 groups in ROI A (Figure 3A; data in Table S4) corresponding to the very early-maturation stage, at which time ameloblasts are smaller and enamel matrix not fully mineralized.[7] The number of ameloblasts in this area was significantly higher in DEHP-treated groups, with 25 ± 5.1 cells for the D-5 groups, 27.8 ± 3.8 cells for the D-50 groups, and only 12.2 ± 1.3 cells for the controls (Figure 3B). Furthermore, the proportion of nonmineralized enamel vs. total enamel thickness was calculated in the area extending from 20 µm-before to 20 µm-after the transition zone (called A). The nonmineralized enamel–matrix was still significantly higher in the DEHP-groups than in the controls, representing $46.8 \pm 7.3\%$ (D-50 group), $44.1 \pm 5.2\%$ (D-5 group), and $30.5 \pm 9.0\%$ (C group), respectively (Figure 3C; data in Table S5).

Mechanical Properties of Teeth of DEHP-Treated Mice

Mechanical properties of early- and late-maturation stage enamel were evaluated by nanoindentation (Figure 4A). All hardness and elastic modulus mean values were lower for DEHP-treated mice than controls over the entire enamel thickness, with the greatest difference recorded at the most external part of the enamel (Figure 4B–D). The control teeth showed hardness and Young's modulus values that increased from the dentin enamel junction (DEJ) to the enamel surface in accordance with previously published data.[42] Mean hardness values (Figure 4B,C; summary data in Table S6) were lower for DEHP-treated mouse enamel than for the control mice by 5–34%, and elastic moduli by 20–44% (Figure 4D,E; summary data in Table S7). There was a dose–response effect for enamel hardness values in early mature enamel, with the greatest differences near the enamel surface (Figure 4B). The hardness values for late-mature enamel (Figure 4C) and elastic moduli for early mature enamel (Figure 4D) were significantly lower than those of the controls. The dose–response was lost for Young's moduli for late-mature enamel, with the D-5 condition showing a stronger reduction than D-50 (Figure 4E). The Young's modulus values were less dispersed in late-mature enamel (Figure 4E) than in early maturation (Figure 4D), with a highly significant difference for more mineralized late-mature enamel ($p < 0.001$) of DEHP-treated mice.

Enamel Gene Expression Profile in Dental Epithelial Cells from Mice or Rat HAT-7 Cells Exposed to DEHP

The expression levels of enamel key genes were measured by RT-qPCR in micro-dissected dental epithelia of control and D-5- and D-50-treated mice. The key genes were regrouped into four major categories that were mRNAs coding for *a*) EMPs: amelogenin (*Amelx*), ameloblastin (*Ambn*), enamelin (*Enam*), and amelotin (*Amtn*); *b*) enamel-specific proteases: metalloprotease 20 (*Mmp20*) and kallikrein 4 (*Klk4*); *c*) ion exchangers required for enamel mineralization and pH regulation: solute carrier family 24 member a4 (*Slc24a4*), solute carrier family 26 member a4 (also called Pendrin; *Slc26a4*), and solute carrier family 5 member a8 (*Slc5a8*); and *d*) steroid receptors possibly involved in the actions of DEHP: androgen receptor (*AR*) and estrogen receptor alpha (*ERα*) (Figure 5A). They were described for their differential expression during amelogenesis, with *Amelx, Ambn, Enam, MMP20, ERα* in the secretory stage and Klk4, *Slc24a4*, *Slc26a4, Slc5a8*, and *AR* in the maturation stage. The levels of mRNAs expressed in the secretory stage of amelogenesis were higher in D-50 than in control dental epithelia, whereas those of genes expressed in the maturation stage were the same or lower: The expression of *Amelx*, *Ambn*, and *Enam* was higher in males treated with DEHP, in a dose-dependent manner, showing significant modulation with 50 µg/kg per day DEHP; $p < 0.05$ (Figure 5A; data in Table S8). Such effects of DEHP were not detected in females (Figure S2). The expression of *Amtn,* which is expressed throughout amelogenesis,[43] remained similar under DEHP treatment. This pattern of modulation (up-regulation of genes expressed in secretory-stage ameloblasts and no change of genes expressed in maturation-stage ameloblasts) was also observed for mRNAs encoding enamel proteases, with the up-regulation of *Mmp20* expression, whereas that of *Klk4* was not affected. To investigate the possible direct effects of DEHP on enamel key gene expression levels in dental epithelial cells, ameloblast-like HAT-7 cells were treated with a large dose range, from 10^{-10} M to 10^{-4} M MEHP (the active metabolite of DEHP),

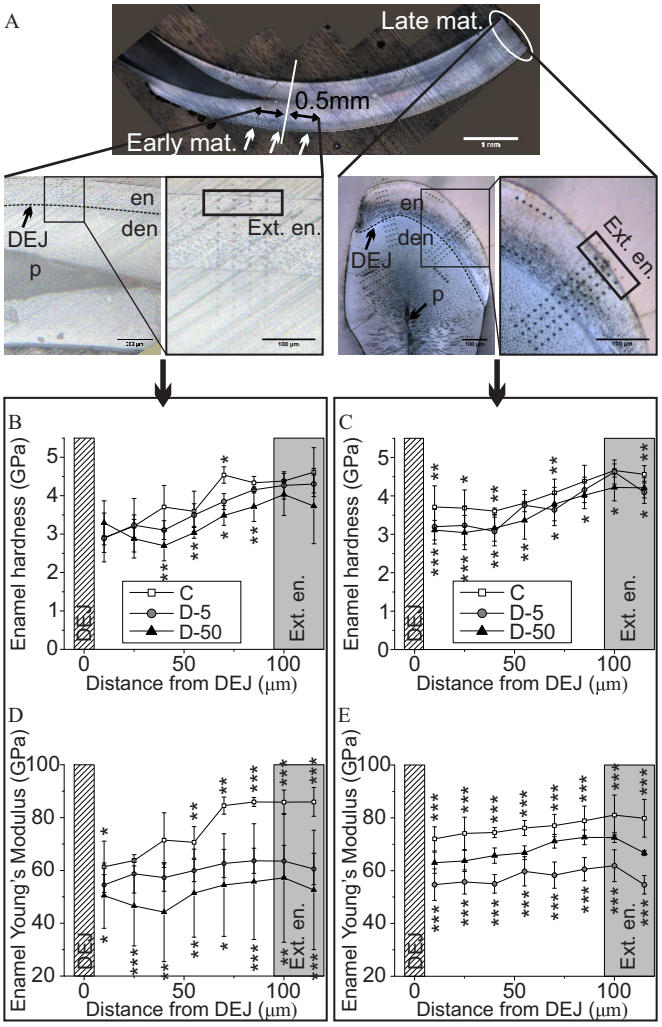

Figure 4. Nano-indentation analysis of control and DEHP-treated male mouse enamel. Comparison of the physical properties of enamel characterized between control mice in white squares, mice exposed to 5 μg/kg BW per day DEHP (D-5 groups) in gray circles and to 50 μg/kg BW per day (D-50 groups) in black triangles. (A) Photographs of nano-indentation measurement points in the incisor, sagittal sections for early mature enamel, and frontal sections corresponding to late mature enamel. Measurements of the hardness of (B) early and (C) late mature enamel respectively, from the DEJ to enamel surface. Young's modulus in (D) early and (E) late mature enamel respectively, from the DEJ to enamel surface. At least three different samples from independent set of experiments were analyzed in each group with at least 90 indent locations per slice ($n = 5$ for control group, $n = 4$ for D-5 group, $n = 5$ for D-50 group). Mean ± SD is shown for graphs. One-way ANOVA analyses with post hoc tests for multiple comparisons with Tukey's correction (*, $p < 0.05$, **, $p < 0.01$, ***, $p < 0.001$ vs. the control group) are indicated. Summary data for (B–E) are available in Table S6 and Table S7. Note: ANOVA, analysis of variance; BW, body weight; C, control; DEHP, di-(2-ethylhexyl) phthalate; DEJ, dentin-enamel junction; den, dentin; en, enamel; Ext.en., external enamel; mat, maturation; p, pulp; SD, standard deviation.

for 48 h (Figure 5B–D; data in Table S9). Although the expression of *Amelx* and *Ambn* were below the level of detection in these cells, both *Enam* (Figure 5B) and *Mmp20* (Figure 5C) mRNA levels showed a dose-dependent higher expression in the MEHP-treated group. The up-regulation was significant for *Enam* from 10^{-6} M MEHP ($p < 0.01$), and from 10^{-8} M MEHP for *Mmp20* ($p < 0.05$).

The mRNA coding for the two steroid receptors, AR and ERα, expressed in dental epithelium[18] were also differentially modulated in tissues exposed to DEHP. Levels of *AR* mRNA, expressed in the maturation stage, were not different, whereas those of *ER*α, which is expressed in the early stages of amelogenesis, were higher in the dental epithelium of DEHP-treated mice (Figure 5A). A similar difference in *ER*α expression (higher compared with control) also occurred in HAT-7 cells treated with 10^{-4} M MEHP, corresponding to a high dose (Figure 5D).

Finally, the levels of expression of the last group of genes investigated here, those encoding ion exchangers, were lower in D-5 groups for *Slc26a4*, and similar for *Slc5a8* (Figure 5A). The levels of *Slc24a4* mRNA showed a dose-dependent higher expression in DEHP-exposed mice.

Discussion

Enamel quality and integrity are important for general health, quality of life, and sociality. They can be affected by inherited genetic characteristics, environmental factors, and lifestyle.[9] The effects of contaminants and pollutants on health are difficult to determine because they are generally present at low doses and metabolized. The oral cavity is one of the main routes of contamination by many toxicants present in food, drinks, and air and by molecules that may leach from dental materials used in dentistry, making oral tissues continually exposed to such molecules. The present study shows how DEHP/MEHP, still present in our environment despite restrictions, affected the development of teeth in mice, causing defects that may alter the quality of life if they also occur in humans. Dental defects are very common and generate onerous costs, increasing social disparities;[44] they thus need to be understood and actively prevented. In addition, the precise characterization of acquired enamel defects will allow their use as early markers of exposure to such molecules.

Exposure to EDCs, including dioxin, BPA, and polychlorinated biphenyls, has been linked to hypomineralizing DDEs in epidemiological[23,24] and in experimental[25,45] studies. EDCs may contribute or aggravate DDEs, as previously described in experimental rodent models.[25,26] Here, we report the analysis of enamel of the continually growing incisors of adult female and male mice chronically exposed to low doses of DEHP. Our data show that the severity of clinically observed dental defects was dependent on the DEHP dose. However, individual susceptibility to DEHP was considerable, with certain animals being highly responsive to D-5, with others presenting no dental alteration to D-50. This is in accordance with current knowledge of the adverse health effects of EDCs[46] and published data on the effects of BPA on rat teeth scored according to severity.[25]

The comparison of dental defects resulting from exposure to DEHP, reported here in mice, and to BPA, reported earlier in rats,[25] highlights a higher prevalence of dental defects in males than in females. First, one explanation could be that males may have a greater need to gnaw on caging than females, which might contribute to the more frequent damage because their incisors are more solicited. However, such events were not observed in controls. Second, another explanation could be that enamel is weaker in males than in females in C57BL/6J strain used in this study. However, despite the limited number of animals included in the study, our observations showed the opposite, with one female with a defective incisor, whereas all males had intact teeth. Such a higher susceptibility of males to DEHP and BPA has also been reported in other experimental pathological contexts, including obesity and brain disorders,[47–49] and in epidemiological studies.[50] The sexual dimorphism has been shown to be associated with sexual steroid hormones, estrogens and androgens, which are also involved in amelogenesis.[16,17] Pro-estrogenic[51] and anti-androgenic[52,53] properties of DEHP have been reported in experimental models. Direct effects of DEHP on AR signaling in the brain without disruption of circulating levels of testosterone have been previously reported in the same animals used in this study.[36] AR is

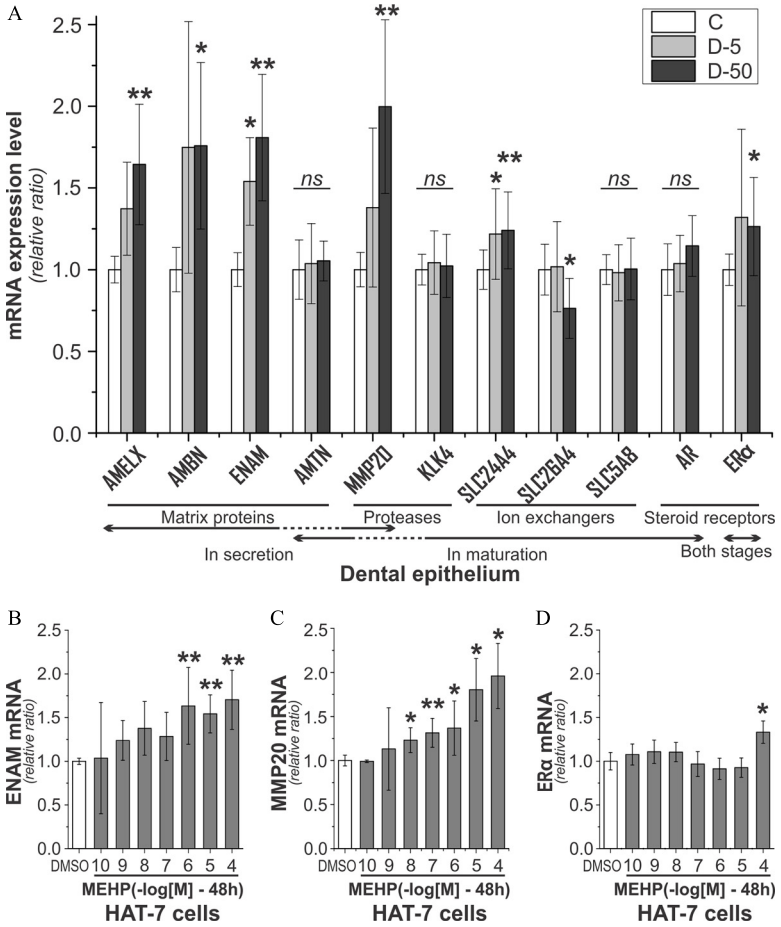

Figure 5. Levels of expression of enamel key genes in dental epithelial cells. (A) Levels of enamel gene expression measured by RT-qPCR of total RNAs prepared from micro-dissected dental epithelia of mice treated with DEHP at 5 µg/kg BW per day (D-5 group; gray columns) and 50 µg/kg BW per day (D-50 group; dark columns) and compared with that of control mice (C group; white columns). (Two RNA extractions/group per set of experiments). The enamel key genes were regrouped into four major categories, which were mRNAs encoding *a*) enamel matrix proteins: amelogenin (*AMELX*), ameloblastin (*AMBN*), enamelin (*ENAM*), and amelotin *(AMTN*); *b*) enamel-specific proteases: metalloprotease 20 (*MMP20*) and kallikrein 4 (*KLK4*); *c*) ion exchangers: solute carrier family 24 member a4 (*Slc24a4*), solute carrier family 26 member a4 (*Slc26a4*), and solute carrier family 5 member a8 (*Slc5a8*); and *d*) sexual steroid receptors: androgen receptor (*AR*) and estrogen receptor (*ERα*). They were differentially expressed during amelogenesis, with *Amelx, Ambn, Enam*, and *MMP20* mainly in the secretory stage; *Klk4*, *Slc24a4*, *Slc26a4, Slc5a8*, and *AR* in the maturation stage; and *ERα* in both stages. Data were adjusted by the mean values of three house-keeping genes [glyceraldehyde-3-phosphate dehydrogenase (*Gapdh*), ribosomal protein S15 (*Rs15*), and TATA-binding protein 1 (*Tbp1*)], used as references. The means were calculated from data measured in three independent experiments ($n = 6$ RNA preparations/group). (B) Expression levels of *Enam* mRNA in rat HAT-7 cells treated with 10^{-10} M to 10^{-4} M MEHP for 48 h. (C) Expression levels of *Mmp20* mRNA in rat HAT-7 cells treated with 10^{-10} M to 10^{-4} M MEHP for 48 h. (D) Expression levels of *ERα* mRNA in rat HAT-7 cells treated with 10^{-10} M to 10^{-4} M MEHP for 48 h were compared with control cells treated with vehicle only (0.1% DMSO). Data were adjusted by the mean values of three house-keeping genes [glyceraldehyde-3-phosphate dehydrogenase (*Gapdh*), Ribosomal protein S15 (*Rs15*), and TATA-binding protein 1 (*Tbp1*)], used as references and graphed relative to control. The means were calculated from triplicates measured in three independent experiments. Means ± SDs are shown for graphs. Values were considered to be significantly different (*) when $p < 0.05$ and highly significantly different (**) when $p \leq 0.01$ by using one-way ANOVA analyses with post hoc tests for multiple comparisons with Tukey's correction. Summary data for (A) are available in Table S8 and for (B–D) in Table S9. Note: ANOVA, analysis of variance; BW, body weight; DEHP, di-(2-ethylhexyl) phthalate; DMSO, dimethyl sulfoxide; MEHP, mono(2-ethylhexyl) phthalate; RT-qPCR, real-time quantitative polymerase chain reaction; SD, standard deviation.

expressed in dental and oral bone cells,[54,55] and such expression may contribute to the overall observed dental defects. However, relations between exposure to DEHP and bone mineralization are still discussed[56] and need to be further investigated. No clear effects of DEHP were observed here in oral bone mineralization of adult mice, despite the DEHP effects previously reported on nonoral bone cells.[34,57] In addition, AR is expressed in maturation-stage ameloblasts,[17] which appeared to be less sensitive to DEHP than secretory-stage ameloblasts, suggesting marginal involvement of AR in the effects of DEHP in enamel. Conversely, ERα may be a good candidate to explain the underlying mechanism of DEHP in dental defects. This receptor is highly expressed in ameloblasts, especially in early stages of amelogenesis,[16,18] which our data showed to be targeted by DEHP. Interestingly, several recent studies have reported ERα and estrogens to be involved in enamel formation and structure in humans[19] and rodents.[58] ERα is involved in preameloblast proliferation,[16] enamel gene expression,[58] and epigenetic regulation.[45]

Given the higher prevalence of dental defects in male mice than in females exposed to DEHP with a dose–response severity, the investigation on their characterization was carried out on males exposed to the highest dose of DEHP. The comparison between BPA effects reported previously in rats[25] and in mice,[45] and DEHP's ability to cause dental defects highlighted alterations in enamel quality, with enamel breakdown and low enamel mineral density, for both molecules. However, such apparently common end points may be due to different causes, with BPA primarily affecting progenitor cell proliferation[25,45] and terminal

enamel mineralization,[17] and DEHP acting earlier, during the transition stage of amelogenesis. DEHP was thus able to delay enamel mineralization as supported by our histology and μCT analyses. Such a delay may explain the lesser enamel rigidity, which in turn predisposed teeth to break when they were subjected to a mechanical stress. Interestingly, the effects of DEHP on enamel mechanical properties were nonmonotonic; such effects have often been reported for EDCs and may explain the individual variability in dental defects clinically observed.[46]

The delay in enamel mineralization is directly related to the synthesis of EMPs, ameloblast differentiation and activity.[9] Although the expression of many genes expressed in maturation-stage ameloblasts (active in terminal enamel mineralization) was either similar or marginally lower compared with control, the expression of many enamel key genes in secretory-stage ameloblasts were higher in DEHP-exposed mice in a dose-dependent manner. These modulations observed *in vivo* in male mice exposed to DEHP may be caused by either direct effects of DEHP on ameloblasts or indirect mechanisms associated to endocrine disruption. This latter hypothesis was refuted because testosterone and estrogen levels remained similar to control levels in our animals that were also studied for their reproductive behavior and sexual hormone levels.[36,37] Conversely, direct dose–response effects of DEHP on ameloblasts were supported by the *in vitro* reproducibility of the modulation of *Mmp20* and *Enam* expression. Interestingly, the expression of these genes was not significantly different in females exposed to DEHP, in accordance with their less pronounced phenotype (Figure S2). Altogether, our results lead us to propose that DEHP up-regulated the expression of genes encoding EMPs in the early stages of amelogenesis, contributing to extend the secretory-stage without sufficient mineralization to compensate for the ongoing eruption.

Despite that the comparison between experimental models and human pathologies is challenging, these experimental data could be translated, at least in part, to humans, who share similar processes of amelogenesis with rodents. Our previous data showed common structural and biochemical features between human DDEs, such as molar incisor hypomineralisation (MIH) and in the enamel of rats exposed to BPA.[25] MIH is a recently described enamel pathology,[59] affecting approximately 15% of 6- to 9-y-old children nowadays,[60,61] with an as-yet unknown etiology.[62] However, recent data reporting an increase the prevalence and severity of MIH reinforce the possibility of environmental conditions as etiological factors for MIH.[63] In addition to EDCs, several other nongenetic causative factors have been proposed—including antibiotics, medications for respiratory diseases and asthma, and anticancer chemotherapy[62]—but none are completely satisfactory. The existence of MIH before the use of amoxicillin[64] and the increased MIH prevalence and severity reported in recent decades argue for the contribution of recent environmental factors. DEHP was found on sampled medical devices in a neonatal intensive care unit,[28] and MIH has also been associated with prematurity and other pathologies in early infancy that require hospitalization.[62] Overall, our results lead us to suggest the involvement of EDCs in enamel hypomineralization and in MIH. However, contrary to our experimental data showing a higher susceptibility of males to DEHP, most of studies report a similar MIH prevalence in boys and girls; using animal models could be a limitation of our study. One explanation could be that DEHP has different effects in humans and rodents because its metabolism is different in humans and rodents,[65] as is the case for many other toxicants with endocrine disrupting activities, such as polyfluoroalkyl substances, for example.[66] Another possible explanation is that MIH may be due to the combination of multiple causal factors. Because humans are exposed to multiple toxicants at a time, which may have different effects depending on the environmental conditions,[67] sex difference may not be observed any more with a mixture. Further analyses on animals exposed to mixtures of EDCs or mother–child cohorts are thus required to determine causal factors of MIH to evaluate the contribution of EDCs in developmental defects of enamel.

Finally, EDCs may have adverse effects on teeth, as well as on other organs, leading to pathological development. The characterization of dental defect selectivity (the type of teeth that are affected provides information on the time-window of exposure to causal agents), color, enamel structure and composition (which may be collected before restoration), and biochemistry in relation with an identified chemical or a mixture, will help to reconstitute the history of exposure. Thus, characterized irreversible developmental dental defects generated during fetal and early postnatal periods may be used as easy noninvasive biomarkers of exposure to environmental enamel disruptors for the early diagnosis of pathologies associated with environmental exposures.[5,40,68,69] For example, MIH, regrouping heterogeneous forms,[70] has been shown to be associated with behavioral disorders[71] and other pathologies, such as celiac disease.[72] Developmental enamel defects associated with various environmental conditions and food intake have also been proposed for the early diagnosis of iron pathologies[40] and mental health risks.[5] In conclusion, our study contributes to the ongoing analysis of enamel defects resulting from exposure to environmental toxicants to reconstitute the history of exposure during the perinatal period of life that is a determinant of adult health.

Acknowledgments

We thank the Centre de Recherche des Cordeliers (CRC) core facilities for the technical and methodological help, assistance and support (CEF). We gratefully acknowledge the Functional Exploration Center staff for technical assistance with the animals. We also acknowledge Christophe Klein (CHIC plateform of the CRC, Paris) for image acquisition.

Micro-CT imaging was performed at the Life Imaging Facility of the Université Paris Cité (Plateforme Imageries du Vivant, Montrouge), supported by France Life Imaging (grant ANR-11-INBS-0006) and Infrastructures Biologie-Santé. The study was funded by the Université Paris Cité, the French National Institute of Health and Medical Research (Inserm), the Fondation Santé Environnementale de la Mutuelle Familiale/Fondation de l'Avenir (grant AP-FSE-17-001 to S.B.), the National Agency for safety of food and environment (grant 2019/1/230 to S.B.), and the Fondation pour la Recherche Medicale (DGE20111123012 to E.V.).

References

1. Braun JM, Sears CG. 2021. Invited perspective: how can studies of chemical mixtures and human health guide interventions and policy? Environ Health Perspect 129(11):111304, PMID: 34817288, https://doi.org/10.1289/EHP10318.
2. Colborn T, Dumanoski D, Myers JP. 1996. *Our Stolen Future: Are We Threatening Our Fertility, Intelligence, and Survival?: A Scientific Detective Story*. New York, NY: Dutton.
3. Gray JM, Rasanayagam S, Engel C, Rizzo J. 2017. State of the evidence 2017: an update on the connection between breast cancer and the environment. Environ Health 16(1):1–61, PMID: 28865460, https://doi.org/10.1186/s12940-017-0287-4.
4. Huhn S, Escher BI, Krauss M, Scholz S, Hackermüller J, Altenburger R. 2021. Unravelling the chemical exposome in cohort studies: routes explored and steps to become comprehensive. Environ Sci Eur 33(1):17, PMID: 33614387, https://doi.org/10.1186/s12302-020-00444-0.
5. Davis KA, Mountain RV, Pickett OR, Den Besten PK, Bidlack FB, Dunn EC. 2020. Teeth as potential new tools to measure early-life adversity and subsequent mental health risk: an interdisciplinary review and conceptual model. Biol Psychiatry 87(6):502–513, PMID: 31858984, https://doi.org/10.1016/j.biopsych.2019.09.030.
6. Rinderknecht AL, Kleinman MT, Ericson JE. 2005. Pb enamel biomarker: deposition of pre- and postnatal Pb isotope injection in reconstructed time points

along rat enamel transect. Environ Res 99(2):169–176, PMID: 16194667, https://doi.org/10.1016/j.envres.2005.01.005.
7. Nanci A. 2012. Enamel: Composition, Formation and Structure. In: *Ten Cate's Oral Histology: Development, Structure and Function*. 8th ed. Maryland Heights, MO: Mosby Elsevier, 122–164.
8. Gerlach RF, Cury JA, Krug FJ, Line SRP. 2002. Effect of lead on dental enamel formation. Toxicology 175(1–3):27–34, PMID: 12049833, https://doi.org/10.1016/S0300-483X(02)00082-3.
9. Lacruz RS, Habelitz S, Wright JT, Paine ML. 2017. Dental enamel formation and implications for oral health and disease. Physiol Rev 97(3):939–993, PMID: 28468833, https://doi.org/10.1152/physrev.00030.2016.
10. Robinson C, Kirkham J, Brookes SJ, Bonass WA, Shore RC. 1995. The chemistry of enamel development. Int J Dev Biol 39(1):145–152, PMID: 7626401.
11. AlQahtani SJ, Hector MP, Liversidge HM. 2010. Brief communication: the London atlas of human tooth development and eruption. Am J Phys Anthropol 142(3):481–490, PMID: 20310064, https://doi.org/10.1002/ajpa.21258.
12. Balic A, Thesleff I. 2015. Tissue interactions regulating tooth development and renewal. Curr Top Dev Biol 115:157–186, PMID: 26589925, https://doi.org/10.1016/bs.ctdb.2015.07.006.
13. Joseph BK, Savage NW, Young WG, Waters MJ. 1994. Prenatal expression of growth hormone receptor/binding protein and insulin-like growth factor-I (IGF-I) in the enamel organ. Anat Embryol (Berl) 189(6):489–494, PMID: 7978354, https://doi.org/10.1007/BF00186823.
14. Lézot F, Descroix V, Hotton D, Mauro N, Kato S, Berdal A. 2006. Vitamin D and tissue non-specific alkaline phosphatase in dental cells. Eur J Oral Sci 114(suppl 1):178–182, PMID: 16674682, https://doi.org/10.1111/j.1600-0722.2006.00338.x.
15. Ferrer VL, Maeda T, Kawano Y. 2005. Characteristic distribution of immunoreaction for estrogen receptor alpha in rat ameloblasts. Anat Rec A Discov Mol Cell Evol Biol 284(2):529–536, PMID: 15803481, https://doi.org/10.1002/ar.a.20190.
16. Jedeon K, Loiodice S, Marciano C, Vinel A, Canivenc Lavier MC, Berdal A, et al. 2014. Estrogen and bisphenol A affect male rat enamel formation and promote ameloblast proliferation. Endocrinology 155(9):3365–3375, PMID: 25004094, https://doi.org/10.1210/en.2013-2161.
17. Jedeon K, Loiodice S, Salhi K, Le Normand M, Houari S, Chaloyard J, et al. 2016. Androgen receptor involvement in rat amelogenesis: an additional way for endocrine-disrupting chemicals to affect enamel synthesis. Endocrinology 157(11):4287–4296, PMID: 27684650, https://doi.org/10.1210/en.2016-1342.
18. Houari S, Loiodice S, Jedeon K, Berdal A, Babajko S. 2016. Expression of steroid receptors in ameloblasts during amelogenesis in rat incisors. Front Physiol 7(Nov):503, PMID: 27853434, https://doi.org/10.3389/fphys.2016.00503.
19. Arid J, Oliveira DB, Evangelista SS, Vasconcelos KRF, Dutra ALT, de Oliveira SS, et al. 2019. Oestrogen receptor alpha, growth hormone receptor, and developmental defect of enamel. Int J Paediatr Dent 29(1):29–35, PMID: 30341791, https://doi.org/10.1111/ipd.12434.
20. Gore AC, Chappell VA, Fenton SE, Flaws JA, Nadal A, Prins GS, et al. 2015. EDC-2: the Endocrine Society's second Scientific Statement on endocrine-disrupting chemicals. Endocr Rev 36(6):E1–E150, PMID: 26544531, https://doi.org/10.1210/er.2015-1010.
21. Le Magueresse-Battistoni B. 2020. Adipose tissue and endocrine-disrupting chemicals: does sex matter? Int J Environ Res Public Health 17(24):1–30, PMID: 33333918, https://doi.org/10.3390/ijerph17249403.
22. Le Magueresse-Battistoni B. 2021. Endocrine disrupting chemicals and metabolic disorders in the liver: what if we also looked at the female side? Chemosphere 268:129212, PMID: 33359838, https://doi.org/10.1016/j.chemosphere.2020.129212.
23. Jan J, Sovcikova E, Kočan A, Wsolova L, Trnovec T. 2007. Developmental dental defects in children exposed to PCBs in Eastern Slovakia. Chemosphere 67(9):S350–S354, PMID: 17250867, https://doi.org/10.1016/j.chemosphere.2006.05.148.
24. Alaluusua S, Lukinmaa PL, Vartiainen T, Partanen M, Torppa J, Tuomisto J. 1996. Polychlorinated dibenzo-*p*-dioxins and dibenzofurans via mother's milk may cause developmental defects in the child's teeth. Environ Toxicol Pharmacol 1(3):193–197, PMID: 21781681, https://doi.org/10.1016/1382-6689(96)00007-5.
25. Jedeon K, De la Dure-Molla M, Brookes SJ, Loiodice S, Marciano C, Kirkham J, et al. 2013. Enamel defects reflect perinatal exposure to bisphenol A. Am J Pathol 183(1):108–118, PMID: 23764278, https://doi.org/10.1016/j.ajpath.2013.04.004.
26. Jedeon K, Houari S, Loiodice S, Thuy TT, Le Normand M, Berdal A, et al. 2016. Chronic exposure to bisphenol A exacerbates dental fluorosis in growing rats. J Bone Miner Res 31(11):1955–1966, PMID: 27257137, https://doi.org/10.1002/jbmr.2879.
27. Braun JM, Sathyanarayana S, Hauser R. 2013. Phthalate exposure and children's health. Curr Opin Pediatr 25(2):247–254, PMID: 23429708, https://doi.org/10.1097/MOP.0b013e32835e1eb6.
28. Calafat AM, Needham LL, Silva MJ, Lambert G. 2004. Exposure to di-(2-ethylhexyl) phthalate among premature neonates in a neonatal intensive care unit. Pediatrics 113(5):e429–e434, PMID: 15121985, https://doi.org/10.1542/peds.113.5.e429.
29. Malarvannan G, Onghena M, Verstraete S, van Puffelen E, Jacobs A, Vanhorebeek I, et al. 2019. Phthalate and alternative plasticizers in indwelling medical devices in pediatric intensive care units. J Hazard Mater 363(Feb):64–72, PMID: 30308366, https://doi.org/10.1016/j.jhazmat.2018.09.087.
30. Monnier P. 2018. Exposure to phthalates of critically ill children: a pilot single center study. Biomed J Sci Tech Res 6(2):2–7, https://doi.org/10.26717/BJSTR.2018.06.001322.
31. Weuve J, Sánchez BN, Calafat AM, Schettler T, Green RA, Hu H, et al. 2006. Exposure to phthalates in neonatal intensive care unit infants: urinary concentrations of monoesters and oxidative metabolites. Environ Health Perspect 114(9):1424–1431, PMID: 16966100, https://doi.org/10.1289/ehp.8926.
32. European Food and Safety Agency Panel on Food Contact Materials, Enzymes and Processing Aids; Silano V, Baviera JMB, Bolognesi C, Chesson A, Cocconcelli PS, et al. 2019. Update of the risk assessment of di-butylphthalate (DBP), butyl-benzyl-phthalate (BBP), bis(2-ethylhexyl)phthalate (DEHP), di-isononylphthalate (DINP) and di-isodecylphthalate (DIDP) for use in food contact materials. EFSA J 17(12):e05838, https://doi.org/10.2903/j.efsa.2019.5838.
33. U.S. Environmental Protection Agency. 2012. *Phthalates Action Plan Summary*. Revised 14 March 2012. https://www.epa.gov/sites/production/files/2015-09/documents/phthalates_actionplan_revised_2012-03-14.pdf [accessed 31 October 2014].
34. Choi JI, Cho HH. 2019. Effects of di(2-ethylhexyl)phthalate on bone metabolism in ovariectomized mice. J Bone Metab 26(3):169–177, PMID: 31555614, https://doi.org/10.11005/jbm.2019.26.3.169.
35. European Union. 2010. Directive 2010/63/EU of the European Parliament and of the Council of 22 September 2010 on the protection of animals used for scientific purposes. Off J Eur Union L 276:33–79.
36. Dombret C, Capela D, Poissenot K, Parmentier C, Bergsten E, Pionneau C, et al. 2017. Neural mechanisms underlying the disruption of male courtship behavior by adult exposure to di(2-ethylhexyl) phthalate in mice. Environ Health Perspect 125(9):097001, PMID: 28934723, https://doi.org/10.1289/EHP1443.
37. Adam N, Brusamonti L, Mhaouty-Kodja S. 2021. Exposure of adult female mice to low doses of di(2-ethylhexyl) phthalate alone or in an environmental phthalate mixture: evaluation of reproductive behavior and underlying neural mechanisms. Environ Health Perspect 129(1):017008, PMID: 33502250, https://doi.org/10.1289/EHP7662.
38. Bazin D, Daudon M. 2015. Les pathologies microcristallines et les techniques de physicochimie: quelques avancées [in French]. Ann Biol Clin (Paris) 73(5):517–534, PMID: 26489810, https://doi.org/10.1684/abc.2015.1070.
39. Molla M, Descroix V, Aïoub M, Simon S, Castañeda B, Hotton D, et al. 2010. Enamel protein regulation and dental and periodontal physiopathology in *MSX2* mutant mice. Am J Pathol 177(5):2516–2526, PMID: 20934968, https://doi.org/10.2353/ajpath.2010.091224.
40. Houari S, Picard E, Wurtz T, Vennat E, Roubier N, Wu TD, et al. 2019. Disrupted iron storage in dental fluorosis. J Dent Res 98(9):994–1001, PMID: 31329045, https://doi.org/10.1177/0022034519855650.
41. Kawano S, Morotomi T, Toyono T, Nakamura N, Uchida T, Ohishi M, et al. 2002. Establishment of dental epithelial cell line (HAT-7) and the cell differentiation dependent on Notch signaling pathway. Connect Tissue Res 43(2–3):409–412, PMID: 12489191, https://doi.org/10.1080/03008200290000637.
42. Zhang YR, Du W, Zhou XD, Yu HY. 2014. Review of research on the mechanical properties of the human tooth. Int J Oral Sci 6(2):61–69, PMID: 24743065, https://doi.org/10.1038/ijos.2014.21.
43. Iwasaki K, Bajenova E, Somogyi-Ganss E, Miller M, Nguyen V, Nourkeyhani H, et al. 2005. Amelotin—a novel secreted, ameloblast-specific protein. J Dent Res 84(12):1127–1132, PMID: 16304441, https://doi.org/10.1177/154405910508401207.
44. Peres MA, Macpherson LMD, Weyant RJ, Daly B, Venturelli R, Mathur MR, et al. 2019. Oral diseases: a global public health challenge. Lancet 394(10194):249–260, PMID: 31327369, https://doi.org/10.1016/S0140-6736(19)31146-8.
45. Li H, Cui D, Zheng L, Zhou Y, Gan L, Liu Y, et al. 2021. Bisphenol A exposure disrupts enamel formation via EZH2-mediated H3K27me3. J Dent Res 100(8):847–857, PMID: 33655795, https://doi.org/10.1177/0022034521995798.
46. Zoeller RT, Vandenberg LN. 2015. Assessing dose–response relationships for endocrine disrupting chemicals (EDCs): a focus on non-monotonicity. Environ Health 14(1):1–5, PMID: 25971795, https://doi.org/10.1186/s12940-015-0029-4.
47. Dagher JB, Hahn-Townsend CK, Kaimal A, Mansi MA, Henriquez JE, Tran DG, et al. 2021. Independent and combined effects of bisphenol A and diethylhexyl phthalate on gestational outcomes and offspring development in Sprague-Dawley rats. Chemosphere 263:128307, PMID: 33297244, https://doi.org/10.1016/j.chemosphere.2020.128307.
48. Sunman B, Yurdakök K, Kocer-Gumusel B, Özyüncü Ö, Akbıyık F, Balcı A, et al. 2019. Prenatal bisphenol A and phthalate exposure are risk factors for male reproductive system development and cord blood sex hormone levels. Reprod Toxicol 87(Aug):146–155, PMID: 31170452, https://doi.org/10.1016/j.reprotox.2019.05.065.
49. Wassenaar PNH, Trasande L, Legler J. 2017. Systematic review and meta-analysis of early-life exposure to bisphenol A and obesity-related outcomes in

rodents. Environ Health Perspect 125(10):106001, PMID: 28982642, https://doi.org/10.1289/EHP1233.
50. Bhandari RK, Deem SL, Holliday DK, Jandegian CM, Kassotis CD, Nagel SC, et al. 2015. Effects of the environmental estrogenic contaminants bisphenol A and 17α-ethinyl estradiol on sexual development and adult behaviors in aquatic wildlife species. Gen Comp Endocrinol 214:195–219, PMID: 25277515, https://doi.org/10.1016/j.ygcen.2014.09.014.
51. Fitzgerald AC, Peyton C, Dong J, Thomas P. 2015. Bisphenol A and related alkylphenols exert nongenomic estrogenic actions through a G protein-coupled estrogen receptor 1 (Gper)/epidermal growth factor receptor (Egfr) pathway to inhibit meiotic maturation of zebrafish oocytes. Biol Reprod 93(6):135, PMID: 26490843, https://doi.org/10.1095/biolreprod.115.132316.
52. Lee HJ, Chattopadhyay S, Gong EY, Ahn RS, Lee K. 2003. Antiandrogenic effects of bisphenol A and nonylphenol on the function of androgen receptor. Toxicol Sci 75(1):40–46, PMID: 12805653, https://doi.org/10.1093/toxsci/kfg150.
53. Carbone S, Ponzo OJ, Gobetto N, Samaniego YA, Reynoso R, Scacchi P, et al. 2013. Antiandrogenic effect of perinatal exposure to the endocrine disruptor di-(2-ethylhexyl) phthalate increases anxiety-like behavior in male rats during sexual maturation. Horm Behav 63(5):692–699, PMID: 23399322, https://doi.org/10.1016/j.yhbeh.2013.01.006.
54. Dale JB, Sarich SL, Bretz TM, Hatton JF, Zachow RJ. 2002. Hormonal regulation of androgen receptor messenger ribonucleic acid expression in human tooth pulp. J Dent Res 81(5):360–365, PMID: 12097452, https://doi.org/10.1177/154405910208100514.
55. Inaba T, Kobayashi T, Tsutsui TW, Ogawa M, Uchida M, Tsutsui T. 2013. Expression status of mRNA for sex hormone receptors in human dental pulp cells and the response to sex hormones in the cells. Arch Oral Biol 58(8):943–950, PMID: 23490353, https://doi.org/10.1016/j.archoralbio.2013.02.001.
56. van Zwol-Janssens C, Trasande L, Asimakopoulos AG, Martinez-Moral MP, Kannan K, Philips EM, et al. 2020. Fetal exposure to bisphenols and phthalates and childhood bone mass: a population-based prospective cohort study. Environ Res 186:109602, PMID: 32668547, https://doi.org/10.1016/j.envres.2020.109602.
57. Bhat FA, Ramajayam G, Parameswari S, Vignesh RC, Karthikeyan S, Senthilkumar K, et al. 2013. Di 2-ethyl hexyl phthalate affects differentiation and matrix mineralization of rat calvarial osteoblasts—*in vitro*. Toxicol In Vitro 27(1):250–256, PMID: 22985736, https://doi.org/10.1016/j.tiv.2012.09.003.
58. Küchler EC, de Lara RM, Omori MA, Schröder A, Teodoro VB, Baratto-Filho F, et al. 2021. Estrogen deficiency affects tooth formation and gene expression in the odontogenic region of female rats. Ann Anat 236:151702, PMID: 33607226, https://doi.org/10.1016/j.aanat.2021.151702.
59. Weerheijm KL. 2003. Molar incisor hypomineralisation (MIH). Eur J Paediatr Dent 4(3):115–120, PMID: 14529330, https://doi.org/10.1159/000047479.
60. Schwendicke F, Elhennawy K, Reda S, Bekes K, Manton DJ, Krois J. 2018. Global burden of molar incisor hypomineralization. J Dent 68(Jan):10–18, PMID: 29221956, https://doi.org/10.1016/j.jdent.2017.12.002.
61. Zhao D, Dong B, Yu D, Ren Q, Sun Y. 2018. The prevalence of molar incisor hypomineralization: evidence from 70 studies. Int J Paediatr Dent 28(2):170–179, PMID: 28732120, https://doi.org/10.1111/ipd.12323.
62. Silva MJ, Scurrah KJ, Craig JM, Manton DJ, Kilpatrick N. 2016. Etiology of molar incisor hypomineralization—a systematic review. Community Dent Oral Epidemiol 44(4):342–353, PMID: 27121068, https://doi.org/10.1111/cdoe.12229.
63. Irigoyen-Camacho ME, Villanueva-Gutierrez T, Castano-Seiquer A, Molina-Frechero N, Zepeda-Zepeda M, Sánchez-Pérez L. 2020. Evaluating the changes in molar incisor hypomineralization prevalence: a comparison of two cross-sectional studies in two elementary schools in Mexico City between 2008 and 2017. Clin Exp Dent Res 6(1):82–89, PMID: 32067391, https://doi.org/10.1002/cre2.252.
64. Garot E, Couture-Veschambre C, Manton D, Beauval C, Rouas P. 2017. Analytical evidence of enamel hypomineralisation on permanent and primary molars amongst past populations. Sci Rep 7(1):1712, PMID: 28490768, https://doi.org/10.1038/s41598-017-01745-w.
65. Hanioka N, Isobe T, Ohkawara S, Ochi S, Tanaka-Kagawa T, Jinno H. 2019. Hydrolysis of di(2-ethylhexyl) phthalate in humans, monkeys, dogs, rats, and mice: an *in vitro* analysis using liver and intestinal microsomes. Toxicol In Vitro 54:237–242, PMID: 30315871, https://doi.org/10.1016/j.tiv.2018.10.006.
66. Fenton SE, Ducatman A, Boobis A, DeWitt JC, Lau C, Ng C, et al. 2021. Per- and polyfluoroalkyl substance toxicity and human health review: current state of knowledge and strategies for informing future research. Environ Toxicol Chem 40(3):606–630, PMID: 33017053, https://doi.org/10.1002/etc.4890.
67. Gaudriault P, Mazaud-Guittot S, Lavoué V, Coiffec I, Lesné L, Dejucq-Rainsford N, et al. 2017. Endocrine disruption in human fetal testis explants by individual and combined exposures to selected pharmaceuticals, pesticides, and environmental pollutants. Environ Health Perspect 125(8):087004, PMID: 28796631, https://doi.org/10.1289/EHP1014.
68. Babajko S, Gayrard V, Houari S, Bui AT, Barouki R, Niederreither K, et al. 2020. La sphère orale, cible et marqueur de l'exposition environnementale [in French]. Med Sci (Paris) 36(3):225–230, PMID: 32228840, https://doi.org/10.1051/medsci/2020024.
69. Babajko S, Lescaille G, Radoï L, Bui AT, Baaroun V, Boyer E, et al. 2020. La sphère orale, cible et marqueur de l'exposition environnementale [in French]. Med Sci (Paris) 36(3):231–234, PMID: 32228841, https://doi.org/10.1051/medsci/2020025.
70. Elhennawy K, Manton DJ, Crombie F, Zaslansky P, Radlanski RJ, Jost-Brinkmann PG, et al. 2017. Structural, mechanical and chemical evaluation of molar-incisor hypomineralization-affected enamel: a systematic review. Arch Oral Biol 83(Nov):272–281, PMID: 28843745, https://doi.org/10.1016/j.archoralbio.2017.08.008.
71. Kohlboeck G, Heitmueller D, Neumann C, Tiesler C, Heinrich J, Heinrich-Weltzien R, et al. 2013. Is there a relationship between hyperactivity/inattention symptoms and poor oral health? Results from the GINIplus and LISAplus study. Clin Oral Investig 17(5):1329–1338, PMID: 22927131, https://doi.org/10.1007/s00784-012-0829-7.
72. Macho VMP, Coelho AS, Veloso e Silva DM, de Andrade DJ. 2017. Oral manifestations in pediatric patients with coeliac disease—a review article. Open Dent J 11(1):539–545, PMID: 29238414, https://doi.org/10.2174/1874210601711010539.